Paper:
Williams, H., Duriez, O., Holton, M., Dell'Omo, G., Wilson, R. & Shepard, E. (2018). Vultures respond to challenges of near-ground thermal soaring by varying bank angle. *The Journal of Experimental Biology*, jeb.174995
http://dx.doi.org/10.1242/jeb.174995

Vultures respond to challenges of near-ground thermal soaring by varying bank angle

Hannah J. Williams*[1], Olivier Duriez[2], Mark D. Holton[1,3], Giacomo Dell'Omo[4], Rory P. Wilson[1], Emily L.C. Shepard[1]

[1]Department of Biosciences, College of Science, Swansea University, Swansea SA2 8PP, UK

2CEFE UMR 5175, CNRS, Université de Montpellier, Université Paul-Valéry Montpellier, EPHE, 1919 route de Mende, 34293 Montpellier Cedex 5, France

[3]Computational Foundry, College of Science, Swansea University, Swansea SA2 8PP, UK

[4] Ornis italica, Piazza Crati 15, 00199 Rome, Italy

*Corresponding author: h.williams@swansea.ac.uk

Keywords: *Gyps* vulture, aeronautical theory, circling envelope, magnetometry, biologging, thermal updraft

Summary statement: Empirical data on soaring behaviour reveal currency trade-offs through the thermal climb.

Thermal soaring birds modulate bank angle

Abstract

Many large birds rely on thermal soaring flight to travel cross-country. As such, they are under selective pressure to minimise the time spent gaining altitude in thermal updrafts. Birds should be able to maximise their climb rates by maintaining a position close to the thermal core through careful selection of bank angle and airspeed, however, there have been few direct measurements of either parameter. Here we apply a novel methodology to quantify the bank angles selected by soaring birds using on-board magnetometers. We couple these data with airspeed measurements to parameterise the soaring envelope of two species of *Gyps* vulture, from which it is possible to predict "optimal" bank angles. Our results show that these large birds respond to the challenges of gaining altitude in the initial phase of the climb, where thermal updrafts are weak and narrow, by adopting relatively high, and conserved, bank angles (25-35°). The angle of bank decreased with increasing altitude, in a manner that was broadly consistent with a strategy of maximising the rate of climb. However, the lift coefficients estimated in our study were lower than those predicted by theoretical models and wind-tunnel studies. Overall, our results highlight how the relevant currency for soaring performance changes within individual climbs; when thermal radius is limiting, birds vary bank angle and maintain a constant airspeed, but speed increases later in the climb in order to respond to decreasing air density.

Introduction

Many large soaring birds rely on thermal updrafts to cover the large distances required to search for food (Ruxton & Houston 2004) or complete long migrations (Alerstam et al., 2003; Judy Shamoun-Baranes et al., 2003; Leshem & Yom-Tov 1996). For the heaviest of these birds, movement across the landscape is completely dependent on their ability to exploit such sources of energy rather than use flapping flight, due to the way that the costs of powered flight scale with body mass (Hedenström & Alerstam 1995; Hedenström 1993). Thermal soaring can be broken down into two different phases; the climb within an updraft, and the glide to the next. In order to maximise the cross-country speed (the overall speed they achieve over ground), birds should

minimise the time in both phases, using different strategies to increase their speed in the glide and their climb rate when soaring. Whilst a wide range of studies has examined the speeds that birds select in inter-thermal glides, and how they vary according to factors such as environmental conditions and experience (Horvitz et al., 2014; Taylor et al., 2016; Harel, Duriez, et al., 2016; Vansteelant et al., 2017), very few studies have examined how individuals maximise their climb rate within a thermal.

The climb rates that can be achieved within thermal updrafts are determined by (i) the morphology of the bird (Pennycuick 2008), (ii) the thermal environment that the bird is soaring within, and (iii) the bird's behavioural response to this environment (Pennycuick 2008; Akos et al., 2010). When it comes to morphology (point (i)), aeronautical models can be used to predict how fast a bird will sink in still air, which changes both with speed (in a manner described by the glide polar) and bank angle (as described by the circling envelope). In order to maximise its climb rate, a bird should fly at its "minimum sink" speed. There are also predictions about the bank angles that birds should adopt. Pennycuick modelled the circling envelopes for soaring birds and calculated the optimal angle of bank for vultures as approximately 24° (Pennycuick 1971; *flight* software (Pennycuick 2009)). Indeed such angles have been observed from gliders (e.g. Shannon et al., 2002) and in Himalayan vultures (*Gyps himalayensis*) flying at low altitudes (Sherub et al., 2016). However, the predicted 24° is arrived at by assuming that birds are aiming to minimise both their turn radius, (and thus remain near the 'core' of the thermal with the strongest uplift) and their sink rate. While this is reasonable when considering how birds should behave on average i.e. that is when considered across thermals, it does not account for the fact that the thermal environment (point (ii) above) changes with altitude. At low altitudes, thermal updrafts are both weak and narrow and we predict that birds should select higher bank angles, with their accompanying higher sink rates, allowing them to exploit stronger uplift closer to the thermal core.

Overall therefore, it is unclear how birds behave given the trade-off between the need to circle tightly, and climb rapidly. This is particularly pertinent in marginal conditions e.g. in the morning when thermals are relatively weak (Spiegel, Getz, et al., 2013; Shannon et al., 2002). The aim of this study was to obtain direct and continuous measurements of bank angle in order to (1) compare these values with theoretical

predictions and (2) ascertain whether and how birds vary their bank angle through the thermal climb. Few studies have quantified bank angle directly, although some in-flight angular measurements have previously been recorded incidentally using on-board cameras, for example to quantify the lateral displacement of the tail in the flight manoeuvers of a Steppe eagle, *Aquila nipalensis* (Gillies et al., 2011). Turning radii can also be derived using GPS data (adjusted for wind drift) or measures of airspeed (Treep et al., 2016; Weinzierl et al., 2016; Horvitz et al., 2014; Sherub et al., 2016). However, deriving bank angle from these measures of turn radius assumes that birds adopt the angles that are required for theoretically ideal circling flight (*cf*. Pennycuick 2008). Here, we use a novel method to quantify bank angle directly, based on an on-board magnetometer, and combine this with measurements of airspeed and circling radii to examine individual variation in soaring behaviour through the thermal climb.

Materials and methods

Study system

Data were collected from four individual vultures (Himalayan griffon vulture, *Gyps himalayensis*, n = 2, European griffon vulture, *Gyps fulvus*, n = 2, all > 2 years) at the Rocher des Aigles falconry centre, Rocamadour, France. Here, vultures were released from their perches to fly freely three times a day (at 11:30, 13:00 and 14:00 local time) in a protocol repeated over three days of data collection, totalling 9 flights for each vulture (see Table 1 for a summary). This protocol provided an opportunity to quantify the flight performance of birds in semi-captive conditions, in a site with relatively good thermal soaring conditions (see Duriez et al., 2014 for details). Wing loading (kg/m^2) was derived from measurements of body mass (kg), and total wing area (m^2) (the latter was calculated from photographs of fully-extended wings on a scaled background), as turning radius increases with wing loading (Akos et al., 2010, Pennycuick 1971).

Device deployment

Vultures were fitted with Daily Diary loggers (DD, recording at 40 Hz) and GPS units (recording position at 4 Hz), which were attached with a Teflon leg-loop harness (Fig. 1) at the beginning of data collection (weight approx. 90 g ~ 1.2% body weight). The harness remained in place for the following 5 days. The harness held an aluminium plate, which was positioned on the lower back, and aligned with the spine. Devices

were attached to the plate using Velcro and were deployed prior to the first flight of the day and were removed at the end of each day. The permit for equipping vultures with loggers was provided as part of the licence of O. Duriez from the Research Centre for Bird Population Studies (CRBPO) of the Natural History Museum (MNHN, Paris). Birds were handled by their usual trainer, under the permit of the Rocher des Aigles.

Daily Diary units (Wilson et al., 2008) were programmed to record the following parameters at 40 Hz; acceleration (*g*) in three axes, geomagnetic field strength (*gauss*), also in three axes, barometric pressure (Pa) and temperature. The DD also incorporated a differential pressure sensor, with dynamic pressure recorded through a forward-facing Pitot tube (brass with a bore diameter of 2.5 mm) that extended outside the housing to measure uninterrupted airflow (see Williams et al., 2015 for details).

Derivation of angle using the magnetometer

Acceleration and barometric pressure data were used to identify the times of take-off and landing (barometric pressure also being used to calculate altitude, see below). It is important to note that while accelerometers could be used to measure postural rotation in many terrestrial systems, they cannot be used to measure bank angle in flight, and in particular soaring flight, due to the centripetal acceleration (see Williams et al., 2015). Thermal soaring flight was defined by a sustained increase in altitude (measured as a decrease in air), the presence of a consistent sine wave in the x- and z-axes of the TriMag data, indicating circling behaviour (Williams et al., 2015) and the distinct lack of flapping (as would be indicated by peaks in dynamic acceleration). Complete turns were selected from all thermal soaring periods; where individual turns were defined as the period between two consecutive peaks in the x-axis.

Estimates of bank angle were derived from the TriMag data as follows, assuming that the bank of the body reflected the bank angle adopted by the wings (this was supported by preliminary work with a camera showing the bank of the wing was consistent relative to the body, Fig. S3). Data from each of the 3 magnetometer channels can be plotted in 3D space and normalised to a spherical surface defined as the *m-sphere* (Williams et al., 2017). Plotting a single 360° rotation for a given bank angle produces an individual ring on the *m-sphere* (Fig. 2). The centroid of this ring, that is, the x, y and z coordinates of the central point of the ring on the surface of the sphere, gives the

158 average bank angle over the course of the complete turn. This was determined by
159 calculating the difference between the dot product of the x, y and z coordinates of a
160 given centroid, and the point of 0° bank (i.e. (0, -1, 0)) using:
161
162 $$\theta = \left(\frac{180}{\pi}\right) * \operatorname{acos}\left[\frac{(0x + -1y + 0z)}{(x^2+y^2+z^2)\sqrt{(0^2+-1^2+0^2)}}\right] \quad \text{Eqn 1}$$
163
164 where x, y and z are the coordinates of the TriMag centroid for a complete turn.
165
166 Plotting the distribution of bank angles estimated using the TriMag approach
167 highlighted skews in the data, suggesting the tags were not perfectly aligned with the
168 sagittal plane of the bird. The exact orientation of the device was not known, and is
169 likely to have differed slightly between birds and days of attachment, causing an
170 overestimation of bank in one direction of turn and an underestimation in the other.
171 Consequently, the data were re-aligned so that the crossing point between turns of
172 opposing direction corresponded to a 0° angle of bank. This therefore assumed that
173 turns of opposing direction had similar ranges in bank angle, analogous to the
174 transformations of Gillies et al., (2011). Centroid angles were recalculated for all flights
175 following realignment. All subsequent analyses of bank angle were made using the re-
176 aligned TriMag data. The processing and analysis of TriMag data were performed with
177 the custom built software DDMT (Wildbytes Technology Ltd., Swansea University).
178
179 *Derivation of soaring parameters*
180 The radius of each complete turn was calculated from the average airspeed of the turn
181 and turn duration. Previous studies have measured turn radius using GPS corrected for
182 wind drift (e.g. Weinzierl et al 2016, Treep et al 2016). By using the airspeed, we can
183 derive radius from the reference frame of the bird, removing the effect of drift on its
184 path. To derive the airspeed, we needed to convert the differential pressure output from
185 volts to true airspeed (V_t) in meters per second. This relationship was derived by
186 selecting 5-second straight-line sections of gliding flight and calculating the airspeed
187 (V_a) in these periods according to the triangle of velocities, using the equation:
188
189 $$V_a{}^2 = V_g{}^2 + V_w{}^2 + 2V_gV_w\cos\gamma \quad \text{Eqn 2}$$
190

where V_g and V_w are the groundspeed (from the 4 Hz GPS) and wind speed vectors respectively, and Υ is the angle between them. The wind vector was specific to each glide, being estimated from drift in the previous thermal just minutes beforehand (via the GPS track by taking the straight-line distance between the corresponding points of complete turns, and dividing by time, see Treep et al., 2016). We used separate linear regressions to calibrate V_t for each bird. These predicted V_t from V_a, *as* well as V_a in interaction with *day* (where significant), to account for the fact that the position of the logger could vary between days. This approach allowed us to determine the airspeed, V_t, at 40 Hz through the entire flight.

The *climb rate* (m/s) per turn was taken as the difference in altitude from the start to the end point of the turn, divided by turn duration; where *altitude* was derived from the barometric pressure (smoothed over 10 seconds), assuming standard atmospheric conditions. The daily mean sea level pressure was taken from the nearest weather station at Lunegarde, 20 km from the study site.

Each individual's circling envelope was parameterised using measured angles of bank (θ) and turn radii (r), and the lift coefficient (C_l), estimated by rearranging:

$$r = \frac{2m}{(C_l * \rho * S * \sin\theta)} \qquad \text{Eqn 3}$$

where m is the mass of the bird (kg), ρ is the air density in 100 m bins following normal conditions, and S is the wing area. Using the median C_l for the bird, we then compared the envelope derived from empirical data to that predicted by Pennycuick's model in *Flight* (Pennycuick 2009). To validate our median lift coefficient we also calculated the C_l in terms of the induced drag (D_i) using the following equations:

$$D_i = mg(sin\varphi) - \frac{1}{2} p {V_t}^2 D_0 S \qquad \text{Eqn 4}$$

$$C_l = \sqrt{\frac{2D_i \pi \mathrm{AR}}{S{V_t}^2 pk}} \qquad \text{Eqn 5}$$

where mg is the weight of the bird, φ is the assumed angle of attack at 15 degrees, ρ is

223 mean air density, V_t is the mean true airspeed, D_0 is the profile drag at Pennycuick's
224 constant of 0.114 (Pennycuick 1971), k is the induced power factor at 1.2 (a commonly
225 used conservative value (see Klein Heerenbrink et al., 2015) that accounts for the wings
226 not being perfectly elliptical) and AR is the aspect ratio.
227
228 *Data analyses*
229 Kruskal-Wallis tests were used to assess individual variation in bank angle and
230 associated climb rate across flights. We examined variation in airspeed with altitude
231 using a linear mixed effects model (LMM) with the random effects of day nested within
232 individual ID. Individual variation in bank angle and climb rate was examined in
233 relation to altitude. Initial inspection of the data suggested that, for each vulture, climb
234 rate levelled off with altitude with a breakpoint in the height at which this occurred. We
235 therefore performed a segmented analysis to identify breakpoints in the individual-
236 specific linear relationships between the climb rate and altitude (R software, *segmented*
237 package (Muggeo 2003)). Data were restricted to ≤ 1000 m for the segmented analysis
238 as birds rarely exceeded this height. The relationship between climb rate and altitude
239 was then compared before and after the identified breakpoint. We did not compare the
240 results in terms of species or age (we did not believe individuals would dramatically
241 differ in soaring performance due to age alone given that all birds were > 2 years; *cf*.
242 Harel, Horvitz & Nathan, 2016), but focused on within-individual trends in climb rate
243 and bank angle, thus allowing us to examine changes in soaring behaviour through the
244 climb. However we did consider the effects of wing-loading on soaring behaviour, as
245 wing loading is the main morphological factor that is known to have significant impact
246 on the limits of the circling envelope.
247
248 Finally, we examined climb rate in relation to distance from the thermal core using the
249 empirically parameterised circling envelope and data collected from a single focal
250 individual (this being the individual where the regression analyses of V_t by V_a accounted
251 for most variance). Assuming a normal distribution of vertical velocities we estimated
252 the maximum climb rate that could be achieved for a given thermal region (i.e. height
253 and radius); partitioning the thermal into low (200 – 400 m), mid (400 – 600 m) and
254 high (600+ m) regions (high being altitudes above the individual's breakpoint, see
255 results). All analyses were performed in R 3.2.3.
256

Results

Overall, 34 flights were recorded across the three days of data collection (*G. himalayensis* 9 flights each, *G. fulvus* 8 flights each, Table 1). Flights ranged from 5.28 to 45.27 minutes (mean = 20.96 ± SD 9.63 minutes). Flights performed in the first release of the day at 11:30 tended to be longer and reach greater altitudes than those of subsequent releases (flight 1: 11:30, 27.04 ± 10.06 minutes, 609.84 ± 323.10 m; flight 2: 13:00, 19.21 ± 6.01 minutes, 424.62 ± 150.38 m; flight 3: 14:30, 14.44 ± 8.82 minutes, 445.86 ± 193.48 m). A total of 1155 complete thermal turns were isolated for bank angle analyses (per individual: 289 ± 70, Table 1). Angles differed significantly between all four individuals (Kruskal-Wallis x^2 = 262.650, df = 3, p<0.001), with median bank angles ranging between 25 and 35° (Table 1). Regression analyses found a significant relationship between V_a (measured from the triangle of velocities) and the raw differential pressure values for each bird, from which conversion equations were derived (Focal Bird A, $V_a = 0.0047 * \text{Pitot} - 28.33$, in a regression with adj.R^2 of 0.71 ; The remaining birds are presented in SupMat1, S1, S2). V_t did not change through the climb when examined in relation to altitude (LMM X^2 = 1.436, df = 5,1, p = 0.231) allowing us to assume a direct relationship between time to complete the turn and its radius (individual airspeeds reported in Table 1).

Overall, birds decreased their bank angle (r = -0.467, N = 1155, p<0.001, Spearman's rank correlation) and increased their turning radius (r= 0.676, N =1155, p<0.001, Spearman's rank correlation) with altitude (Fig. 3), in a manner consistent with a movement along the circling envelope. There was also a general increase in climb rate with altitude, with l significant break in this relationship for each of the four individuals (Table S1, the average breakpoint was 560 ± 41 m across all birds). The relationship between climb rate and altitude was highly conserved before the breakpoint (e.g. for the bird shown in Fig. 3: r = 0.637, N = 218, p < 0.001), but variable, and with a lack of correlation, after the breakpoint (r = -0.025, N = 116, p = 0.792, Table 2).

The birds occupied a space within their theoretical circling envelope as predicted by the theoretical maximal lift coefficient (Fig. 4A). In fact, the overall agreement was very good, in terms of the empirical data being apparently bounded by the theoretical envelope. However, there was some variation in sink rate for a given combination of circling radius and bank angle, with birds operating below their theoretical optima (i.e.

291 at a lower lift coefficient). This decrease in performance did not seem to be related to
292 the wind vector (Fig. 4B) or the time or day of the flight. Instead, it is likely to reflect
293 the relatively high airspeeds adopted by these birds, which were typically 13-14 m/s,
294 compared to the predicted minimum sink speeds of up to 9 m/s.
295
296 The lift coefficients that birds generally operated at were lower than the theoretical C_l
297 at minimum sink (ranging from 1.37 to 1.47), irrespective of the method used. When
298 the empirical values of bank angle and turn radius were used, average lift coefficients
299 were estimated to be 0.73 and 0.83 for the *Gyps fulvus* individuals and 0.79 and 0.82
300 for the *Gyps himalayensis*. The C_l calculated from the biometric data, average airspeed
301 and Pennycuick's drag constants, was equally low e.g. 0.81, for the focal bird (Fig. 4A).
302 The consequences of the lower C_l, mean that this individual had an average limiting
303 turn radius of 13.68 m, compared to a radius of 7.9 m with a theoretical C_l of 1.37.
304
305 **Discussion**
306
307 In this study we use novel techniques to measure bank angle and turn radius using
308 animal-attached loggers. Our method of obtaining bank angle capitalises on the
309 inherently three-dimensional nature of magnetometry data, which can be normalised to
310 the surface of a sphere (when measurements are made in all 3 axes). We show that, for
311 a complete turn in thermal soaring, the rotation in heading defines a circular ring on the
312 sphere, and the position of this ring is determined by the animal's posture (Williams et
313 al., 2017). As vultures show relatively little variation in pitch during thermal soaring,
314 changes in the position of the circle result from rotation in the roll axis. The use of 3-
315 dimensional magnetometry data therefore allows us to quantify bank angle for
316 prolonged periods of time, with the advantages of minimal calibration and post
317 processing in comparison to camera methods (used here to validate the magnetometry
318 method in preliminary analyses). Gyroscopes in on-board devices can also be used to
319 measure angular movement (e.g. Martín López et al., 2016; Noda et al., 2014; Wilson
320 et al., 2013), in practice however, gyroscopes are not well suited to continuous data
321 collection on free-living animals, due to their relatively high current draw (a problem
322 that also limits the use of cameras).
323

Early work by Pennycuick (1971) proposed that *Gyps* vultures should adopt bank angles of between 20 and 40°. Our measurements generally align with these theoretical predictions, in terms of the median bank angles adopted. Nonetheless, birds were somewhat conservative in the maximum angles they used. That is, while they tended to select angles up to 35°, they could, according to the theoretical circling envelope, increase their bank angles by a further ~5° before incurring substantial penalties in sink rate. Adopting tight turning radii may be associated with the risk that small control inputs could cause a bird to 'overbank' and move into an area of performance space with high sink rates, thus compromising climb performance. This is the first work that does not assume that these birds are operating at the limits of their performance, but rather, examines the distribution of data within the circling envelope to investigate within-individual variation in performance, an approach that could be developed further to provide insight into individual strategies or interspecific variation. It is interesting to note that the adult female maintained average climb rates at least 25% greater than other birds, as well as the lowest variance in bank angle overall. This increased performance and consistency may be an indicator of soaring skill acquired through greater experience (*cf*. Harel, Horvitz & Nathan, 2016).

Thermal updrafts tend to be narrower and weaker when close to the ground, expanding as they rise. Optimising soaring performance at low altitudes is therefore critical in order to gain sufficient altitude to glide to the next thermal (Pennycuick 2008). Indeed, it has been recognised since the 1960s (e.g. Kruuk 1967) that the activity rhythms of soaring birds are determined by the mass of the bird in relation to the strength of thermal updrafts, with larger birds only able to gain altitude later in the day when thermals are stronger (*cf*. Spiegel, Getz, et al., 2013). Birds in this study displayed marked changes in bank angle with altitude, decreasing from around 30° to 22° in the first few hundred metres of the climb, and increasing their turn radii in a manner generally consistent with the circling envelope (i.e. the optimal solution for climbing performance). The relatively tight relationship between bank angle, climb rate and altitude in the first few hundred metres, demonstrates the importance of changes in bank angle in enabling soaring birds to gain altitude when close to the ground.

Our finding that birds modulate radius by changing bank angle is in contrast to that of a recent study on Himalayan griffon vultures soaring in excess of 6000 m (Sherub et

al., 2016). While the Himalayan griffons also increased their radius with altitude, they achieve this by increasing their airspeed (keeping bank angle constant). This increase in radius and airspeed is necessary to compensate for the decreasing air density over a dramatic altitudinal range. Interestingly therefore, soaring birds appear to vary their circling radius by two different mechanisms according to the flight altitude. This dual strategy demonstrates the complexity involved in maximising height gain and leads to the question of when and how birds should switch strategy through the climb. With little height above the ground, the priority has to be maximising the climb rate. It seems most likely that birds increase their airspeed at, or above, the point when thermal radius is no longer the primary constraint.

In our system there was a breakpoint in the relationship between climb rate and altitude at some 560 m. As turn radius increases, birds experience diminishing returns in sink rate. Vertical velocity above the breakpoint is therefore less likely to be linked to variation in bank angle, but rather the thermal conditions, which may also vary between days. Since the birds used here do not roam far during their flights, it could also be that they have no need to gain height beyond that required to return to their home destination. Nonetheless, we see no clear advantage in maintaining, rather than increasing altitude, should the thermal structure allow (though see Shannon et al., 2002).

While the variation in bank angle with altitude that we observed was consistent with a tendency to maximise the climb rate, the average lift coefficient was 52% of the theoretical maximum (it is also less than the C_l observed for a jackdaw soaring at its minimum sink speed in a wind tunnel e.g. Rosén & Hedenström, 2001). Our measurements of C_l could have been influenced by factors that fall into three main categories: i) methodological, ii) environmental and iii) behavioural (Fig. 5). In terms of the methodology, while a low lift coefficient may be the result of an overestimated bank angle or turning radius (the latter could result from an over-estimated airspeed), the fact that our data did not cross the theoretical circling envelope supports the idea that they are accurate, as do our data checks, which resulted in an equally low lift coefficient. When it comes to behaviour, these birds were often recorded flying at airspeeds that were higher than the theoretically predicted minimum sink speeds (which is also likely linked to their conservative bank angles, see above). Actual flight speeds

were more similar to those recorded in inter-thermal glides in previous work (recorded at an average of 16.5 m/s by Harel, Duriez et al., (2016)), which could therefore explain the low C_l values. In terms of environmental parameters, we found no clear relationship between wind or time of day, and position within the envelope. However, while there was no evidence of the C_l varying with wind strength, it may be that wind affects soaring performance in a complex way (e.g. Harel, Horvitz & Nathan, 2016).

Overall, we show that the constraints on soaring flight vary with altitude, and that this results in birds modulating their circling radius in relation to two different factors. At low altitudes, obligate soaring birds select relatively steep bank angles to maintain their position in a narrow region of strong uplift (Fig. 5). However, while the circling envelope appeared to be predicted well by theoretical models, we demonstrate that it cannot be assumed that soaring birds are operating at their theoretical optima, and that performance may be influenced by additional factors. Longer term data from free-ranging individuals could provide insight into how the bank angles selected during the critical, near-ground phase of soaring may vary with experience (*cf*. Harel, Horvitz & Nathan, 2016) and state variables such as hunger (Nathan et al., 2012; Spiegel, Harel, et al., 2013), which may provide an incentive for birds to operate in more marginal conditions or select higher bank angles.

Acknowledgments

We would like to thank all the D. Maylin and R. Arnaud directors at the Rocher des Aigles (Rocamadour, France) and all of their staff for their patience and interest in the project. We are extremely grateful to Eric and his team for their enthusiasm, keen interest in the project and willingness to work this data collection protocol into their daily routine. We also thank S. Potier and J. Fluhr for their help with tag deployments. DD housings were designed by P. Hopkins. HJW was funded by a Swansea University Studentship and would also like to thank C. Rees-Roderick for fruitful discussions.

Competing interests

All authors declare no competing interests.

Funding

HJW was supported by a Swansea University studentship during data collection through to completion of the manuscript.

Data Availability

All data collected from the onboard devices can be accessed in the Movebank study *Gyps vultures with Pitot airspeed at Rocamadour* and are to be published in the Movebank data repository with DOI 10.5441/001/1.4f03k6s5

References

Akos, Z., Nagy, M. & Vicsek, T. (2010). Thermal soaring flight of birds and unmanned aerial vehicles. *Bioinspiration & biomimetics*, 5(4), p.045003.

Alerstam, T., Hedenström, A. & Åkesson, S. (2003). Long-distance migration: evolution and determinants. *Oikos*, 103(2), pp.247–260.

Duriez, O. et al. (2014). How Cheap Is Soaring Flight in Raptors? A Preliminary Investigation in Freely-Flying Vultures. *PLoS ONE*, 9, p.e84887.

Gillies, J.A., Thomas, A.L.R. & Taylor, G.K. (2011). Soaring and manoeuvring flight of a steppe eagle Aquila nipalensis. *Journal of Avian Biology*, 42, pp.377–386.

García-Ripollés, C., López, López P. & Urios, V. (2011). Ranging behavioru of non-breeding Eurasian Griffon Vultures Gyps fulvus: a GPS-telemetry study. Acta Ornithologica. 46(2), pp,127-134.

Harel, R., Duriez, O., et al. (2016). Decision-making by a soaring bird: time, energy and risk considerations at different spatio-temporal scales. *Philosophical Transactions of the Royal Society of London B: Biological Sciences*, 371(20150397).

Harel, R., Horvitz, N. & Nathan, R. (2016). Adult vultures outperform juveniles in challenging thermal soaring conditions. *Scientific Reports*, 6(27867).

Hedenström, A. (1993). Migration by soaring or flapping flight in birds: The relative importance of energy cost and speed. *Philosophical Transactions of the Royal Society B*, 342(1302).

Hedenström, A. & Alerstam, T. (1995). Optimal flight speed of birds. *Philosophical Transactions of the Royal Society B*, 348, pp.471–487.

Horvitz, N. et al. (2014). The gliding speed of migrating birds: slow and safe or fast and risky? *Ecology Letters*, 17(6), pp.670–679.

Klein Heerenbrink, M., Johansson, L.C. & Hedenström, A. (2015). Power of the wingbeat: modelling the effects of flapping wings in vertebrate flight. Proceedings of the Royal Society A. 471(2177)

Kruuk, H. (1967). Competitoin For Food Between Vultures in East Africa. *Ardea*, 55(3-4), pp.171–193.

Leshem, Y. & Yom-Tov, Y. (1996). The use of thermals by soaring migrants. *Ibis*, 138(4), pp.667–674.

Martín López, L.M. et al. (2016). Tracking the kinematics of caudal-oscillatory swimming: a comparison of two on-animal sensing methods. *The Journal of Experimental Biology*.

466 Muggeo, V.M.R. (2003). Estimating regression models with unknown break-points.
467 *Statistics in medicine*, 22, pp.3055–3071.

468 Nathan, R. et al. (2012). Using tri-axial acceleration data to identify behavioral modes
469 of free-ranging animals: general concepts and tools illustrated for griffon
470 vultures. *The Journal of experimental biology*, 215(Pt 6), pp.986–96.

471 Noda, T. et al. (2014). Animal-mounted gyroscope/accelerometer/magnetometer: In
472 situ measurement of the movement performance of fast-start behaviour in fish.
473 *Journal of experimental marine biology and ecology*, (451), pp.55–68.

474 Pennycuick, C.J. (2009). Flight. Available at:
475 http://www.bristol.ac.uk/biology/research/staff/penycuick.c.html.

476 Pennycuick, C.J. (1971). Gliding flight of the white-backed vulture Gyps Africanus.
477 *journal of experimental biology*, 55, pp.13–38.

478 Pennycuick, C.J. (2008). *Modelling the Flying Bird. Vol. 5* 1st Editio., Boston:
479 Elsevier.

480 Rosén, M. & Hedenström, A. (2001). Gliding flight in a jackdaw: A wind tunnel
481 study. The Journal of Experiemental Biology, 204, pp.1153-1166.

482 Ruxton, G.D. & Houston, D.C. (2004). Obligate vertebrate scavengers must be large
483 soaring fliers. *Journal of Theoretical Biology*, 228(3), pp.431–436.

484 Schneider, C.A., Rashband, W.S. & Eliceiri, K.W. (2012). NIH Image to ImageJ: 25
485 years of image analysis. *Nature Methods*, 9(7), pp.671–675.

486 Shamoun-Baranes, J. et al. (2003). Differential use of thermal convection by soaring
487 birds over central Israel. T*he Condor*, 105, pp.208–218.

488 Shamoun-Baranes, J. et al. (2003). Using a convection model to predict altitudes of
489 white stork migration over central Israel. *Boundary-Layer Meteorology*, 107,
490 pp.673–681.

491 Shannon, H.D. et al. (2002). American white pelican soaring flight times and altitudes
492 relative to changes in thermal depth and intensity. *The Condor*, 104, pp.679–683.

493 Shepard, E.L.C. et al. (2011). Energy beyond food: Foraging theory informs time
494 spent in thermals by a large soaring bird. *PLoS ONE*, 6(11), p.e27375.

495 Sherub, S. et al. (2016). Behavioural adaptations to flight into thin air. *Biology*
496 *Letters*, 12, p.20160432.

497 Spiegel, O., Harel, R., et al. (2013). Mixed strategies of griffon vultures' (Gyps
498 fulvus) response to food deprivation lead to a hump-shaped movement pattern.
499 *Movement Ecology*, 1(5).

500 Spiegel, O., Getz, W.M. & Nathan, R. (2013). Factors influencing foraging search
501 efficiency: Why do scarce lappet-faced vultures outperform ubiquitous white-
502 backed vutlures. *The American Naturalist*, 181(5), pp.E102–E115.

503 Taylor, G.K., Reynolds, K. V. & Thomas, A.L.R. (2016). soaring energetics and glide
504 performance in a moving atmosphere. *Philosophical transactions of the Royal*
505 *Society of London. Series B, Biological sciences*, 371(1704).

506 Treep, J. et al. (2016). Using high-resolution GPS tracking data of bird flight for
507 meteorological observations. *Bull. Amer. Meteor. Soc.*, 97, pp.951–961.

508 Vansteelant, W.M.G. et al. (2017). Soaring across continents: decsion-making of a
509 soaring migrant under changing atmospheric conditions along an entire flyway.
510 *Journal of Avian Biology*, Online.

511 Weinzierl, R. et al. (2016). Wind estimation based on thermal soaring of birds.
512 *Ecology and Evolution*, 6(24), pp.8706–8718.

513 Williams, H.J. et al. (2015). Can accelerometry be used to distinguish between flight
514 types in soaring birds? *Animal Biotelemetry*, 3(1), p.45.

515 Williams, H.J. et al. (2017). Identification of animal movement patterns using tri-axial
516 magnetometry. *Movement Ecology*, 5(6).

517 Wilson, A.M. et al. (2013). Locomotion dynamics of hunting in wild cheetahs.
518 *Nature*, 498, pp.185–189.

519 Wilson, R.P., Shepard, E.L.C. & Liebsch, N. (2008). Prying into the intimate details
520 of animal lives: Use of a daily diary on animals. *Endangered Species Research*,
521 4(1-2), pp.123–137.

522 **Figure legends**

523

524

525 **Fig. 1. Griffon vulture in flight, wearing a leg loop harness and tags (Daily Diary; GPS)**

526

527

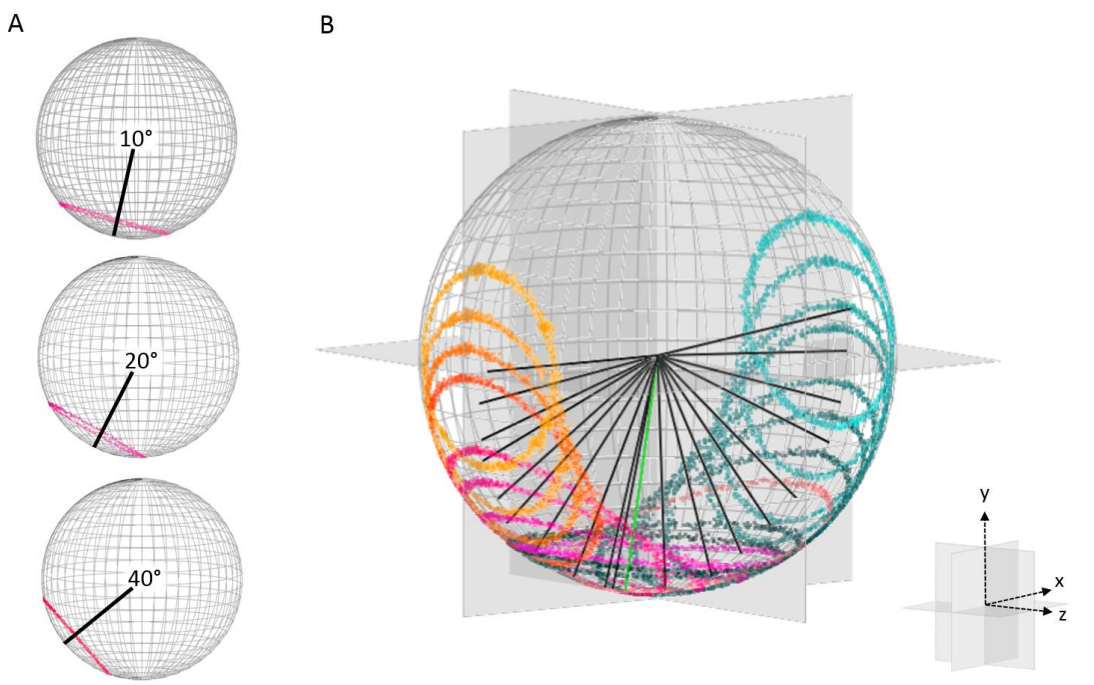

528

529 **Fig. 2. Tri-axial magnetometry data normalised to a spherical surface (the *m-sphere*).** (A)
530 Complete rotations of the magnetometer appear as circles on the sphere, with the line from the
531 centre of the *m-sphere* to the centroid of each circle indicating the mean angle of bank in a
532 given turn. (B) A calibration device was used to simulate a bird circling with fixed bank angles
533 varying from -90 (yellow) to 90°s (light blue) at 10° intervals, indicative of left and right banked
534 turns respectively. The *m-print* that corresponds to zero bank is at the bottom of the *m-sphere*.
535 Units were calibrated using this device in the field, with the camera and GPS units also attached
536 to the platform (as these could potentially influence the magnetometer data (*cf*. Bidder et al.,
537 2015)).

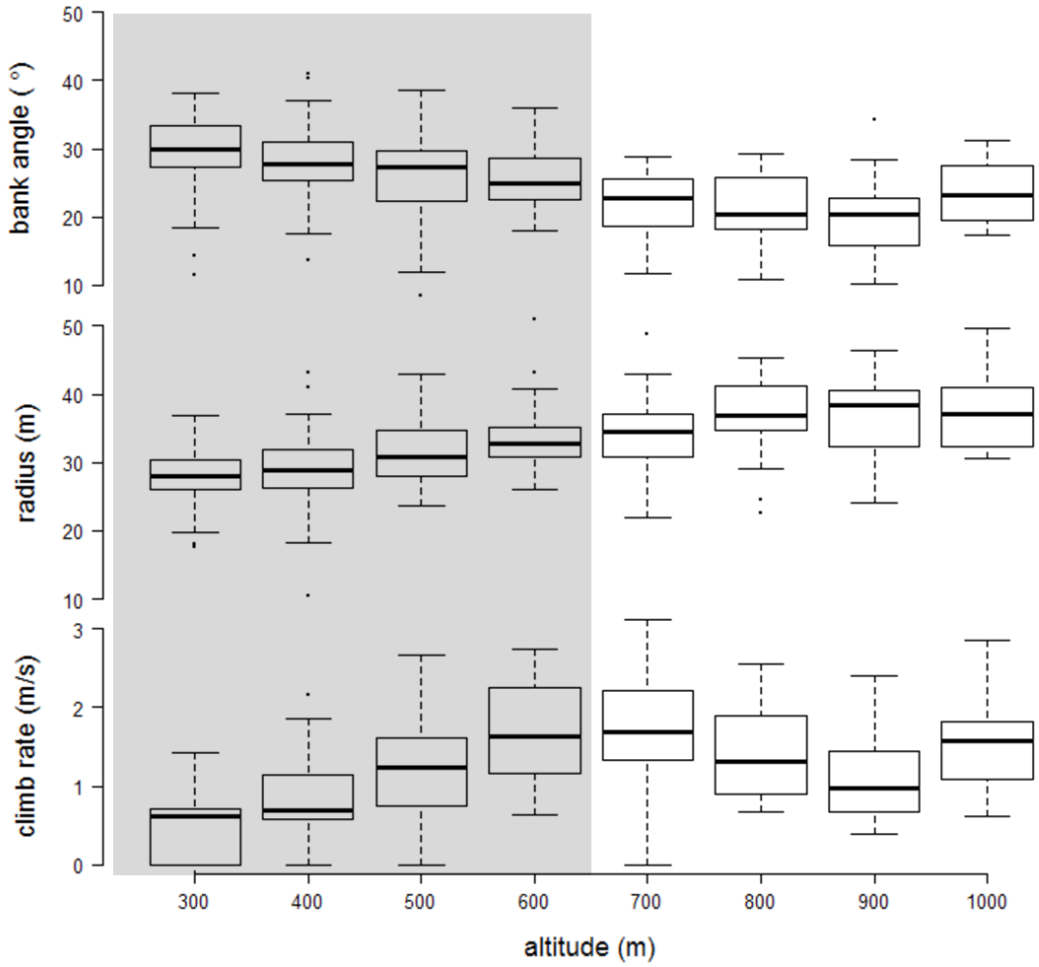

Fig. 3. Trends in the angle of bank, turning radius and the achieved climb rate, binned according to altitude ASL (100 m bin width) **for the *Gyps himalayensis* subadult**. The shaded region highlights the low altitude region below the modelled breakpoint for this bird (515.91 ± 22.86 m) where an increase in climb rate occurred as birds decreased their bank angle (n = 334). This trend does not hold beyond the breakpoint in any bird (Table S1).

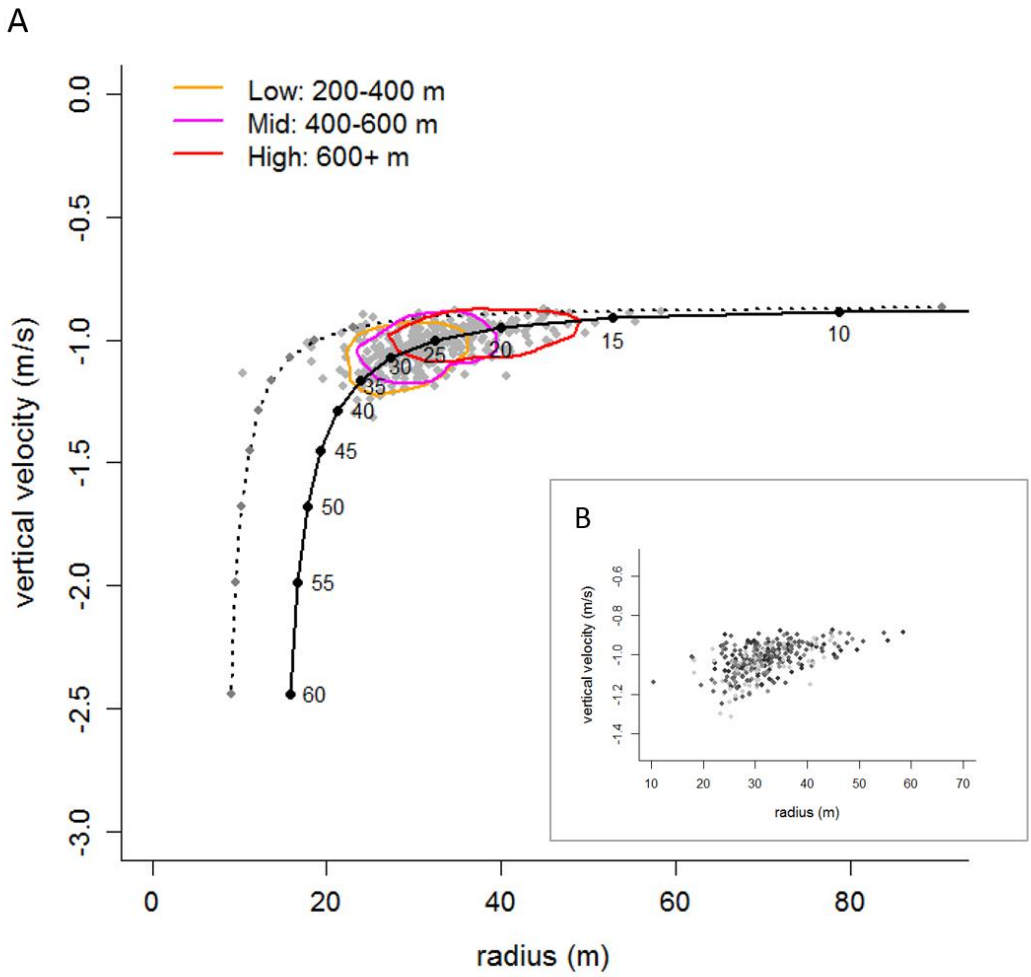

544

545 **Fig. 4. The circling envelope for vulture A, the *Gyps himalayensis* subadult,** (A)
546 parameterised using empirical data (grey dots) of bank angle and turning radius (n = 334)**.** With
547 increasing radius and decreasing bank angle the birds own sink rate decreases (labelled as
548 negative vertical velocity). The bird shifts along this envelope from high bank angles and tight
549 turning radii to a region of low angles and greater turning radii, decreasing its sink rate with
550 altitude (0.9 polygons). Although the empirical data sit within the envelope predicted by the
551 Pennycuick model (dotted line) (Pennycuick 2008, 2009), which assumes a C_l of 1.37, actual
552 turning radii were greater than predicted for a given angle of bank. This produces a higher
553 estimate of the average limiting turn radius (13.68 m), given a median coefficient (C_l) of 0.79.
554 (B) The relationship between sink rate, bank angle and turning radius does not appear to be
555 related to wind speed (gradient of light to dark grey with increasing wind speed).

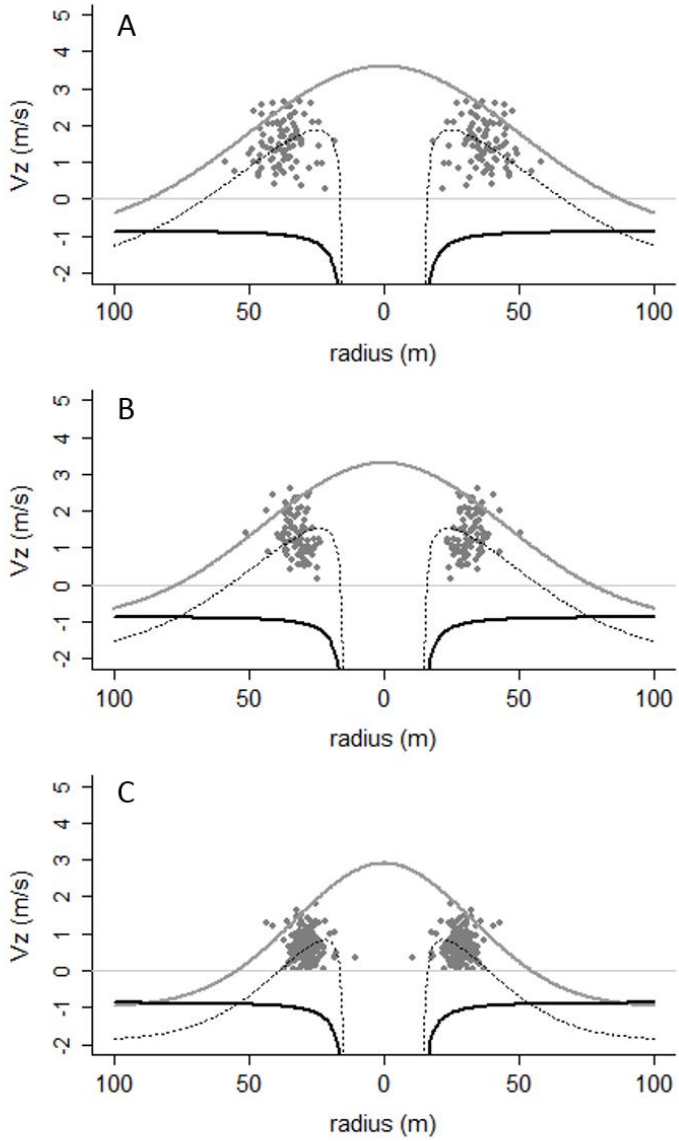

Fig. 5. The velocity profile of a thermal updraft at three altitudes, as modelled from the climb rates, radii and circling envelope for the *Gyps himalayensis* subadult. When soaring, the thermal's upward vertical velocity (solid dark grey line) exceeds that of the birds' downward velocity, so that the bird experiences a positive climb rate. Hence the thermal velocity is taken as the sum of the bird's mean climb rates (raw data shown by grey points) and estimated sink rates for three regions: A) high: 600+m, B) mid: 400-600 m and C) low: 200-400m. This is then interpolated across the thermal diameter assuming a normal distribution of uplift. The bird's circling envelope (solid black line), and the rate at which air is rising within the thermal, define the area within which the bird is able to position itself and gain height. This area is where the climb rate (dotted line) > 0 m/s (horizontal line). Achievable climb rates drop dramatically close to the core of the updraft due to the sink rates associated with high bank angles.

569 **Table 1. Summary flight statistics for the four tagged vultures.** The number of flights and
570 total flight time include all time spent in the air, all other flight parameters are specific to the
571 thermal soaring periods. Average values are given as the mean ± SD, and as the median ±
572 IQR for climb, bank and C_l. For the number of flights and complete turns, values are given for
573 the three release times through the day (a) 11:30 local time, (b) 13:00 and (c) 14:30.
574

Individual	**A**	**B**	**C**	**D**
Species	*Gyps himalayensis*	*Gyps himalayensis*	*Gyps fulvus*	*Gyps fulvus*
Sex	Female	Female	Male	Male
Age	Subadult	Adult	Subadult	Subadult
Wing loading	**6.63**	**7.18**	**7.06**	**7.28**
Body mass (kg)	**8.45**	**8.10**	**7.20**	**7.15**
Wing area (m^2)	**1.27**	**1.13**	**1.02**	**0.98**
Aspect ratio	**5.98**	**6.95**	**6.73**	**6.88**
Nº Flights	(a) 3 (b) 3 (c) 3	(a) 3 (b) 3 (c) 3	(a) 3 (b) 3 (c) 2	(a) 3 (b) 3 (c) 2
Total flight (min)	22.01 ± 10.35	26.77 ± 9.17	17.45 ± 9.83	17.59 ± 7.49
Prop. of circling	54 ± 10 %	49 ± 9 %	54 ± 6 %	51 ± 7 %
Max altitude (m)	847.72 ± 380.88	898.20 ± 334.01	702.93 ± 382.14	707.24 ± 350.35
Nº complete turns	(a) 146 (b) 73 (c) 115 Total = 334	(a) 122 (b) 122 (c) 115 Total = 359	(a) 131 (b) 92 (c) 32 Total = 255	(a) 85 (b) 84 (c) 38 Total = 207
Climb rate (m/s)	**0.99 ± 0.90**	**1.25 ± 1.21**	**0.91 ± 0.99**	**0.83 ± 0.82**
Bank angle (°)	**26.54 ± 7.58**	**29.38 ± 7.29**	**31.74 ± 8.29**	**35.78 ± 10.24**
Average Airspeed (m/s)	**13.21 ± 0.03**	**13.51 ± 0.03**	**12.89 ± 0.05**	**14.15 ± 0.09**
Lift Coefficient (C_l)	**0.79 ± 0.20**	**0.82 ± 0.20**	**0.94 ± 0.23**	**0.73 ± 0.17**

575

576 **Table 2. Relationship between climb rate and altitude before and after the identified**
577 **breakpoint in the climb.** Spearman's rank correlation test for low and high thermal regions
578 (significant relationships in bold) using data prior to and following the break points identified
579 from their corresponding models (Table S1).
580

Bird ID	Break Point (m)	
A	509.85 ± 26.18	**Low: r = 0.621, N = 214, p < 0.001** High: r = -0.024, N = 120, p = 0.792
B	463.13 ± 32.83	**Low: r = 0.582, N = 206, p < 0.001** **High: r = 0.261, N = 153, p = 0.001**
C	680.17 ± 69.56	**Low: r = 0.451, N = 212, p < 0.001** High: r = -0.069, N = 43, p = 0.657
D	607.00 ± 72.17	**Low: r = 0.398, N = 180, p < 0.001** High: r = -0.049, N = 27, p = 0.806

581
582

583 **Supplementary Material**

584

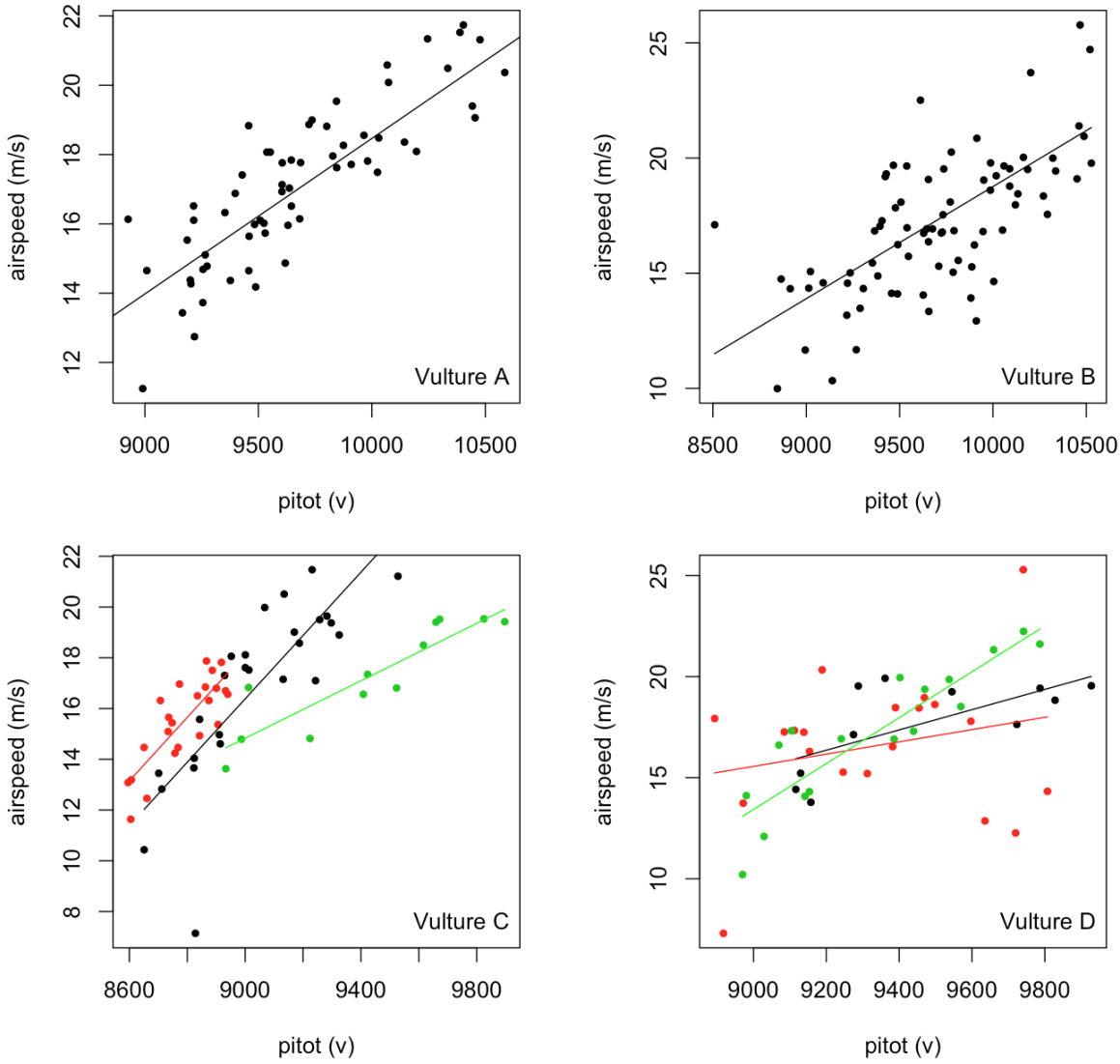

585

586 **Figure S1: regression of the Pitot tube airflow against airspeed derived from the**
587 **wind and ground speed vectors in gliding**. Vulture A (no interaction with day, Adj
588 R^2 =0.71), Vulture B (no interaction, but independent effect of day, Adj R^2 = 0.56),
589 Vulture C (interactive effect of day, Adj R^2 = 0.67), Vulture D (interactive effect of
590 day, Adj R^2 = 0.33).

591

592 We performed individual-specific linear regressions that predicted airspeed values (V_a)
593 from the corresponding Pitot tube data (volts) and used the relationship outputs to
594 convert volts to metres per second values for all data collected during the glides.
595

Vulture A		$V_a = 0.004700\mathrm{P} - 28.33$	Eqn. 1
		adj.R2 = 0.7102, F = 150.5,df=1,60, p <0.001	
Vulture B		$V_a = 0.004865\mathrm{P} - 29.88864$	Eqn. 2
		adj.R2 = 0.56, F = 34.63, df = 3,75, p<0.001	
Vulture C	Day 1	$V_a = 0.01248P - 95.94$	Eqn. 3a
	Day 2	$V_a = 0.0125130\mathrm{4}P - 94.464$	Eqn. 3b
	Day 3	$V_a = 0.005662P - 36.13$	Eqn. 3c
		adj.R2 = 0.67, F = 25.6, df = 5,55, p<0.001	
Vulture D	Day 1	$V_a = 0.005014P - 29.766782$	Eqn. 4a
	Day 2	$V_a = 0.00303\mathrm{4}P - 11.74594$	Eqn. 4b
	Day 3	$V_a = 0.011\mathrm{3}\mathrm{5}\mathrm{3}P - 88.74803$	Eqn. 4c
		adj.R2 = 0.33, F = 5.55, df = 5,42, p<0.001	

596
597

598 **Table S1. Segmented models for climb rate by altitude** for each individual.
599 Spearman's rank correlation tests between climb rate and altitude are also given; for
600 low and high thermal regions using data prior to and following the break points
601 identified from their corresponding models.

Bird ID	variable	estimate	Std. error	t	P
A	Intercept	-0.886	0.209	-4.248	<0.001
(Gaelle)	x	0.005	0.001	8.407	<0.001
	u1.x	-0.005	0.001	-7.880	NA
	Adjusted R^2 = 0.383; 4 interactions for convergence				
Estimated break point: 509.85 ± 26.18 m					
Low: r = 0.621, N = 214, p < 0.001; High: r = -0.024, N = 120, p = 0.792					
B	Intercept	-0.827	0.266	-3.109	0.002
(Giselle)	x	0.005	0.001	6.633	<0.001
	u1.x	-0.004	0.001	-5.335	NA
	Adjusted R^2 = 0.361; 3 interactions for convergence				
Estimated break point: 463.13 ± 32.83 m					
Low: r = 0.582, N = 206, p < 0.001; High: r = 0.261, N = 153, p = 0.001					
C	Intercept	-0.402	0.172	-2.340	0.020
(Gregoire)	x	0.004	0.000	7.808	<0.001
	u1.x	-0.003	0.001	-4.300	NA
	Adjusted R^2 = 0.450; 3 interactions for convergence				
Estimated break point: 680.17 ± 69.56 m					
Low: r = 0.451, N = 212, p < 0.001; High: r = -0.069, N = 43, p = 0.657					
D	Intercept	-0.700	0.260	-2.694	0.008
(Hector)	x	0.004	0.001	6.075	<0.001
	u1.x	-0.004	0.001	-2.737	NA
	Adjusted R^2 = 0.330; 2 interactions for convergence				
Estimated break point: 607.00 ± 72.17 m					
Low: r = 0.398, N = 180, p < 0.001; High: r = -0.049, N = 27, p = 0.806					

602
603
604

Figure S3: composite of wing to body position during thermal soaring. Screenshots taken from a camera placed on top of our tag device attached to the lower back of the bird, with the camera facing the tip of the right wing. Video was recorded on multiple days from two different birds and through different thermal climbs, and the shots taken at random. The image clearly shows consistency in the body-to-wing position within and between climbs, and interestingly this was also evident between climbs of differing turn direction. Though they may be capable of changing wing orientation at the shoulder joint, if they did so predominantly in soaring we would expect clockwise turns that show the ground to show very little wing in the image, and anti-clockwise turns where the wing is pointing towards the sky, to fill the image with the wing.